ARTICLES

Separation of spin and charge excitations in one-dimensional $SrCuO_2$

C. Kim* and Z.-X. Shen
Department of Applied Physics and Stanford Synchrotron Radiation Laboratory, Stanford University, Stanford, California 94305

N. Motoyama, H. Eisaki, and S. Uchida
Department of Superconductivity, The University of Tokyo, Yayoi 2-11-16, Bunkyo-ku, Tokyo 133, Japan

T. Tohyama
Department of Physics, Faculty of Education, Mie University, Tsu 514, Japan

S. Maekawa†
Department of Applied Physics, Nagoya University, Nagoya 464-01, Japan
and Institue for Materials Research, Tohoku University, Sendai 980-77, Japan
(Received 23 January 1997; revised manuscript received 28 May 1997)

In this paper we expand on our earlier results [Phys. Rev. Lett. **77**, 4054 (1996)] on angle-resolved photoemission studies on one-dimensional $SrCuO_2$ that reveal a behavior of a hole in Cu-O chain. The results cannot be explained within the conventional band theory, but require a picture in which the spin and charge degrees of freedom for a single electron are separated. Instead of a single branch as predicted in band theory, E versus k relationship can be explained by underlying spinon and holon excitations scaled by hopping energy t and exchange energy J, respectively, indicating separated spin and charge excitations. This is an experimental observation of direct consequence of the spin-charge separation driven by electron correlations that was first predicted thirty years ago. It also shows spinon and holons are real particles with definite energy-momentum dispersions. [S0163-1829(97)07244-5]

Almost thirty years ago, in their now famous study of the one-dimensional (1D) Hubbard model, Lieb and Wu laid a foundation for the discovery of a new quantum phenomenon called spin-charge separation.[1] This and succeeding theoretical investigations found that the low-energy excitations in a 1D system are not quasiparticles with charge e and spin 1/2 as in an ordinary Fermi liquid. Instead, they are decoupled collective modes of spin and charge excitations called spinons and holons.[2] The decoupled nature of the excitations leads to different speed for spin and charge propagation. This is naturally interpreted as the separation of the spin and charge degrees of freedom for a single electron, or equivalently, a decay of a hole into a holon and a spinon. This novel concept has received renewed interest, largely due to the recent attempts to understand high-T_c superconductors in the context of strongly correlated electron systems.[3–5]

An experimental investigation of this phenomenon is of conceptual significance for several reasons. First, it provides a very strong test for the many-body theoretical model Hamiltonians that are extensively used to describe highly correlated electron systems. The solution of these Hamiltonians are well accepted in one dimension. A comparison of experiment and theory thus provides a quantitative test for the models. Second, if spin-charge separation does occur in one dimension, holons, and spinons can be considered as new elementary particles in solids with similar conceptual importance as that of phonons and magnons. Furthermore, the knowledge we gain about spinons and holons in one dimension will be valuable for us to assess the contention that spin-charge separation occurs in two dimensions. Motivated by these goals, several attempts have been made to detect the spin-charge separation using photoemission spectroscopy.[6–8] To date, however, these studies of 1D metallic samples have not yielded any unambiguous evidence for spin-charge separation.[9]

Recently, high-quality single crystals of a new family of 1D antiferromagnetic (AF) insulators, such as $SrCuO_2$ and Sr_2CuO_3, became available. For low-energy excitations, these materials can be modeled by chains of atoms with one electron per site. Two electrons can not occupy the same site because of the strong on-site Coulomb repulsion, thus making an otherwise metal into an insulator. The electrons on the neighboring sites interact with each other through the antiferromagnetic exchange interaction J. The insulating nature and large exchange interaction value J make these materials ideally suited to detect the spin-charge separation effect.[10] Figure 1 depicts a simplified picture of the spin-charge separation in such a half-filled 1D antiferromagnetic insulator. When an electron is kicked out by a photon, it leaves a hole behind it. Hopping of this hole to a neighboring site, or equivalently, hopping of a neighboring electron into the hole site, creates a magnetic excitation (marked as a wavy line in the figure). However, additional hopping in the same direction does not create magnetic excitations. The motion of the

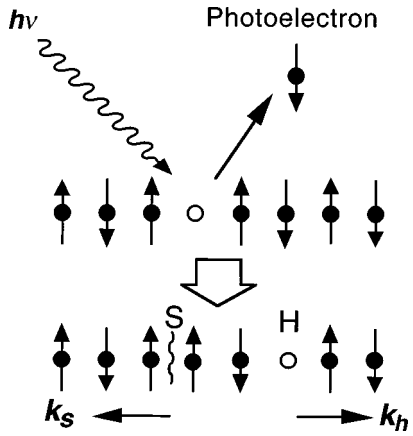

FIG. 1. Photoemission process in a chain with short-range AF ordering. A photohole created in the photoemission process decays into a spin excitation (spinon, labeled as *S*) and a charge excitation (holon, labeled as *H*). The spinon and holon propagate independently with different speeds.

charge vacancy is free from magnetic interaction aside from the first step. Therefore, the original single photohole decays into two separate ''defects'' in the chain, marked as *H* and *S*. The motion of the charge *H* is governed by the hopping energy *t* and the propagation of the magnetic excitation *S* is governed by exchange interaction *J*. Propagating with two different speeds, these two defects can be regarded as two separate particles (that is, spin and charge are separated) and they give the essence of a holon and a spinon. Thus, even without going into too much detail for the moment, we know that the spin-charge separation will manifest itself with a mixture of two branches of dispersive bands due to two particles with different interaction energies.

Earlier we reported observation of spin-charge separation of a photohole in 1D antiferromagnetic insulator $SrCuO_2$.[11] In this paper we report expanded studies on the material. Unlike its 2D counterpart $Sr_2CuO_2Cl_2$, where only a band of width scaled by *J* plus higher-energy tail is observed,[12] a distinct band of width scaled by *t*, which is about three times of *J* as observed. This result is completely different from what one would expect from the band theory that predicts the 1D bandwidth to be half of the 2D bandwidth. Detailed polarization analysis of the data yields multiple branches of dispersive bands for momenta from 0 to 0.5, but only a single band from 0.5 to 1 (in units of π/a with *a* being the Cu-O-Cu distance). The widths of the upper and lower bounds of the bands from 0 to 0.5 can be explained by underlying bands scaled by *t* and *J*, respectively, while the width of the band from 0.5 to 1 is scaled by *t*. These otherwise incomprehensible results can be naturally and quantitatively explained by many-body theoretical calculations, naturally incorporating the spin-charge separation concept without any free parameters. We believe these results constitute a direct observation of the spin-charge separation.

As shown in Fig. 2, $SrCuO_2$ has a weakly coupled double Cu-O chain structure.[13] The important structural character of $SrCuO_2$ is that it has 180° Cu-O-Cu bonds that form the chains and the almost 90° Cu-O-Cu bonds that give the coupling between the chains. The coupling along the chains is at least an order of magnitude stronger than the interchain coupling, making $SrCuO_2$ a 1D compound.[13,14] Single crystals of

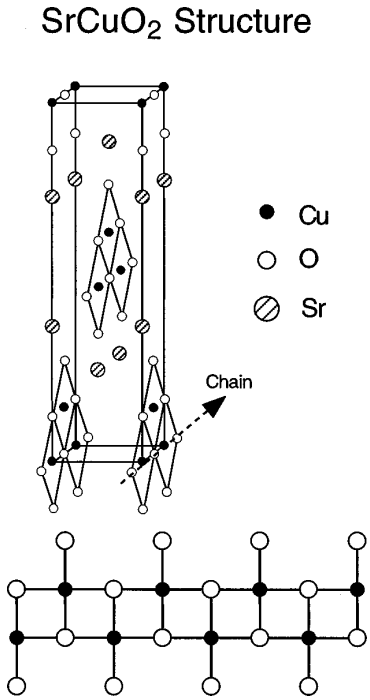

FIG. 2. The unit cell of $SrCuO_2$. The arrow shows the chain direction. The double chain structure is also shown in the figure. Note that hopping between chains has to go through 90° Cu-O-Cu bonding in contrast to 180° Cu-O-Cu bonding along the chains. Orthogonality of oxygen p_x and p_y orbitals suppresses the interchain hopping.

$SrCuO_2$ were grown by the traveling solvent floating zone method. For the experiments, the crystals were cleaved with the Cu-O-Cu chains parallel to the surface. In angle-resolved photoemission spectroscopy (ARPES) experiments, electrons in a solid are excited above the vacuum level by incident monochromatic photons, and the energy and the emission angle of the emitted electrons are measured by an analyzer. In the case of a 1D compound like $SrCuO_2$, the conservation laws imply a simple one to one mapping between the electron emission angle and its momentum inside the solid, facilitating a detailed mapping of the *E* versus *k* relationship along the chain.[15] The room-temperature ARPES data presented here were obtained using a VSW (Vacuum Science Works) system attached to the undulator beamline 5-3 of SSRL (Stanford Synchrotron Radiation Laboratory), at a base pressure of 5×10^{-11} torr. With 22.4 eV photons, the total energy resolution was typically 70 meV, and the angular resolution was $\pm1°$.

Panels (a) and (b) of Fig. 3 present ARPES data from $SrCuO_2$ with the momentum along the chain $k_\parallel$ spanning 0 to 1 as indicated by the numbers associated with each curve. Dispersive features are clearly observed in the data as $k_\parallel$ changes from 0 to 1. On the other hand, we observed minimal dispersion when the momentum perpendicular to the chains ($k_\perp$) varies with $k_\parallel$ fixed (not reported here), consistent with the notion that the electronic structure is mainly determined by $k_\parallel$ because of the 1D nature of $SrCuO_2$.[16] This internal check was carried out at $k_\parallel=0.5$, where the peak is sharpest and thus it is easiest to see any possible dispersion. Other than the strongly dispersive peak, we observe steplike features near $k_\parallel=1.0$ around 17.5 eV kinetic energy, which we attribute to backgrounds. This signal is weak and is iden-

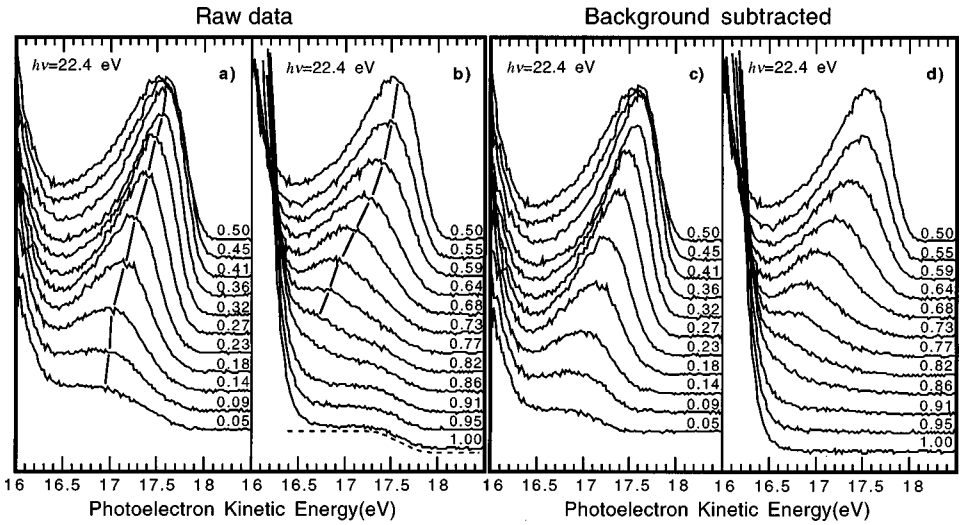

FIG. 3. ARPES data on $SrCuO_2$. The number on each spectrum shows the momentum parallel to the chain in units of π/a where a is the Cu-to-Cu distance along the chain. The data set 1 (a and b) are raw data taken with the electron momentum perpendicular to the chains ($k_\perp$) of 1 and the photon polarization parallel to the chain direction. The lines are a guide to the eye for the peak positions. Panels c and d show the data after the background (dashed line) has been subtracted as discussed in the text.

tical for spectra recorded at $k_\parallel$ ranging from 0.91 to 1.0, in contrast to the data recorded for $k_\parallel$ near 0.05. This behavior strongly indicates that the steplike signal seen near $k_\parallel = 1.0$ is the background due to scattered electrons. This steplike background has been extensively observed in cuprate superconductors when the band has crossed the Fermi level.[15] Further evidence for this signal being the background is the empirical anticorrelation between its intensity and surface quality observed in our data. Since the background signal is approximately isotropic, we subtracted a steplike background (shown as dashed line) from all the spectra, yielding the data in panels (c) and (d).

With the increase of $k_\parallel$ from 0 to 1, a well-defined structure shows a strong dispersion with a maximum near $k_\parallel = 0.5$. For $k_\parallel$ from 0 to 0.5, the feature disperses upwards by about 0.6 eV. Beyond $k_\parallel = 0.5$, the feature disperses more rapidly backwards with a larger extrapolated total dispersion of more than 1 eV. This is better visualized in panel (a) of Fig. 4 in which we replot the data in Fig. 3 in color scale. The dashed line traces the peak positions of the spectra that were shown in Fig. 3. It reveals the asymmetry of the dispersion with respect to $k_\parallel$ of 0.5. Panel (b) of Fig. 4 shows another set of spectra. The differences in experimental conditions for data in panels (a) and (b) are that we changed the polarization of the photons and the momentum perpendicular to the chains. Since we observed minimal $k_\perp$ dispersion, the effects of such changes are expected to be mostly on the modulation of photoemission intensities due to matrix element changes, but not on the electronic structure (that is, the peak position). The dashed line again shows the peak positions. It is apparent at first glance that the dispersion is symmetric with respect to $k_\parallel = 0.5$. The dispersion between $k_\parallel = 0$ and $k_\parallel = 0.5$ is quite different from that of panel (a) while the dispersion in 0.5 to 1 range is very similar.

Figure 5 shows the experimental E versus $k_\parallel$ relations constructed from the two sets of data in Fig. 4 together with

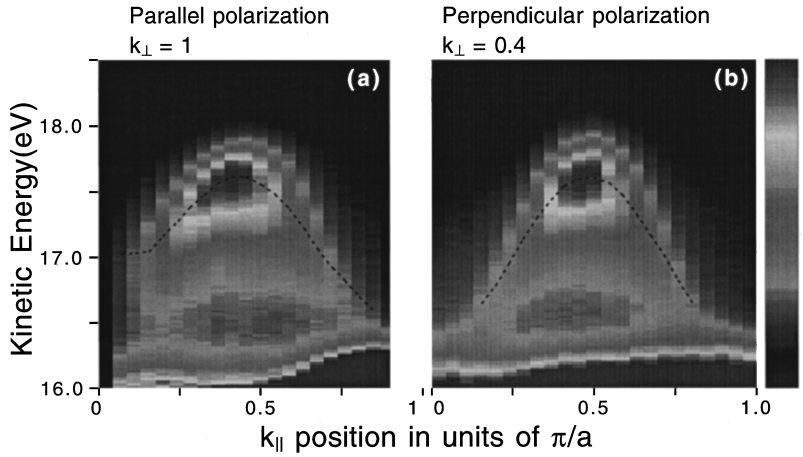

FIG. 4. (a) The density plot of the data shown in Figs. 3(c) and 3(d). The color scale on the right-hand side of the figures shows the intensity. The dashed line traces the peak positions. There is a clear asymmetry between 0 to 0.5 and 0.5 to 1. The high-intensity region at the bottom of the figure is the main valence band. (b) The density plot of the data taken with $k_\perp = 0.4$ and perpendicular polarization.

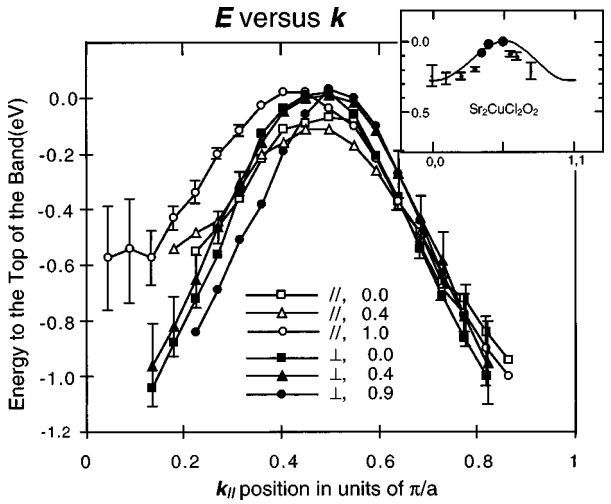

FIG. 5. E vs $k_{\|}$ relations for different polarization and $k_{\perp}$ combinations. $\|$ and $\perp$ indicate parallel and perpendicular polarizations, respectively. The numbers show the $k_{\perp}$ momenta in units of π/a. Error bars are presented only for the two data sets shown in Fig. 4. Also shown in the inset is the (0,0) to (1,1) cut on $Sr_2CuO_2Cl_2$ for comparison (from Ref. 12).

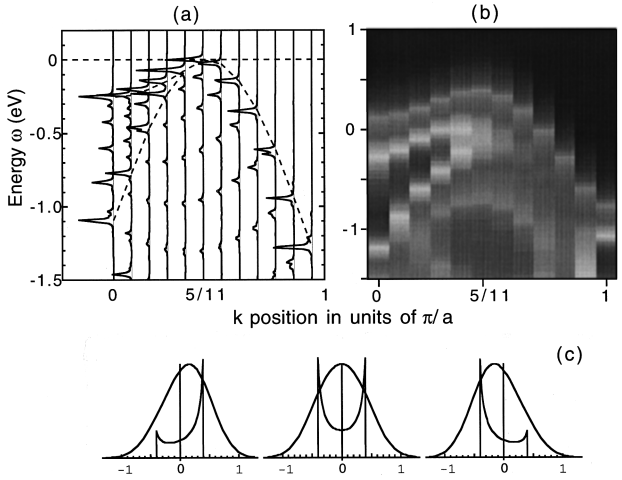

FIG. 6. (a) The calculated spectral function $A(k,\omega)$ in the t-J model with a ring of 22 sites. $J=0.2$ eV and $t=0.6$ eV were used. The energy ω is measured from the highest-energy peak at $k=5/11$. The edge with spinon (holon) character is marked with red (blue) dashed line. Several peaks seen between the two edges rather than continuous spectra are due to a finite-size effect. (b) The density plot of (a) after convoluted with a Gaussian of which the width is extracted from the experimental data. (c) A simulation of modulation effects on the observed peaks. The curves with two-edge structure simulate the broad spectra expected between $k=0$ and 0.5 when infinite number of sites are used in the calculation. Even though two-edge structure is never observed, intensity modulation of the two branches moves the resulting peak positions.

four additional sets of data recorded with other combinations of polarization and $k_{\perp}$. The energy positions are evaluated from the maximum spectral intensity. For clarity, error bars are presented only for the two sets of data in Fig. 4. This plot highlights the asymmetry of the dispersion relationship with respect to $k_{\|}$ of 0.5. For $k_{\|}$ between 0 and 0.5, multiple branches are possible with their band widths ranging from 0.6 eV to more than 1 eV. From 0.5 to 1, the dispersion curves collapse into a single band of width more than 1 eV. The fact that the bands collapse into a single branch in $k_{\|}$ range between 0.5 and 1 further ensures that the spread of bands in $k_{\|}$ range between 0 and 0.5 is not due to $k_{\perp}$ dispersion and that the interchain coupling is very small. It also excludes the possibility of experimental errors. For comparison, the inset in the figure shows the dispersion for 2D $Sr_2CuO_2Cl_2$ along the (1,1) direction.[12] The size of the filled circles represent the spectral weight at each k point. There are two important aspects of this data in contrast to 1D data. First, the overall bandwidth is only about 0.3 eV. Second, there is a sudden intensity drop across the (0.5,0.5) position.

The experimental data in Figs. 3, 4, and 5 cannot be explained within the framework of the conventional band picture. First, the data show that $SrCuO_2$ is an insulator with the band maximum at $k_{\|}=0.5$ while the band theory predicts it to be a metal. Second, as shown in the inset of Fig. 5, the bandwidth of more than 1 eV observed here is at least three times wider than the 0.3 eV bandwidth observed in the 2D Cu-O plane compound $Sr_2CuO_2Cl_2$ whose CuO_2 planes are made of the same Cu-O-Cu bonds.[12] Because the structure and the length of Cu-O-Cu bonds in the 1D and 2D cases are almost identical (less than 2% difference), band calculations would predict that the bandwidth for the 1D compound is half of that of the 2D compound. On very general grounds, band theory predicts the bandwidth for a 1D compound is $2t$ while that for a 2D compound is $4t$.[17] Therefore, the ratio of the widths of the distinct bands observed in 1D and 2D cases is a factor of 6 different from what one expects from the band theory.[18] Third, the band picture predicts no bands between 0.5 and 1. By contrast, the data show a single band with very strong spectral weight in that region. One may argue that there are bands only in the region between 0 and 0.5, and the spectral weight seen between 0.5 and 1 is a shadow band due to AF ordering or a spin density wave. However, the shadow band effect is very weak even when it exists, as seen in the 2D insulator. Finally, aside from the splitting due to the interchain coupling, which is expected to be very small, one expects only a single band between 0 and 0.5 from the band theory. The fact that we see multiple bands in the region cannot be reconciled with the band picture.

The striking contrast of our results with that of the band picture reveals the exotic nature of the data from $SrCuO_2$. Now we try to explain the data using many-body models. While the intellectually related Hubbard and t-J models are both capable of explaining our data, we will discuss the data using the t-J model because both t and J can be obtained by other means, so that there are no free parameters in the theory. Both models can explain the insulating nature of $SrCuO_2$ as a consequence of correlation effects. We chose a rounded value of 0.2 eV for J based on magnetic[13] and optical[20] measurements. The hopping integral t of about 0.6 eV can be obtained from the ratio $t/J=3$, the ratio for other cuprates. Figure 6(a) shows the results of an exact diagonalization t-J model calculation of the spectral functions, $A(k,\omega)$, for 22 sites.[21] Discrete peaks seen in the figure are due to the finite-size effect. One would expect a continuous broad spectrum from infinite site calculation. There is a clear similarity between the numerical calculation results and the data. From 0 to 0.5, there are broad excitations with the two

most intense edge branches scaled by $1.6J$ and $2t$, respectively. On the other hand, there is only one edge branch scaled by $2t$ between 0.5 and 1. Detailed numerical analysis of charge and spin correlation functions shows that the excitation of width $2t$ is due to charge (holon band) while that of width $1.6J$ is due to spin (spinon band).[11] Therefore, a mixture of spinon and holon excitations are possible from 0 to 0.5.

To make a comparison easier, we broaden the theoretical data with the experimental peak width obtained at $k_{\|}=0.5$ where the peak is the sharpest.[22] From the broadened plot in Fig. 6(b), it is immediately clear that we should not be able to resolve the spinon and holon branches as different peaks as in the theory curve. Yet, there is a good overall agreement between the theory and the experiment. The much larger dispersion (compared to the 2D case) and the asymmetry of the dispersion with respect to $k_{\|}=0.5$ seen in the data from the 1D compound can be quantitatively explained by the underlying excitations of holons and spinons scaled by t and J, respectively. These are the direct consequences of the spin-charge separation and are most important experimental observations that cannot be understood in a conventional band picture even at a qualitative level. This contrast in the ability to explain the observed dispersion relationships is the strongest evidence for spin-charge separation.

Photoemission matrix modulation may explain why the maximum spectral intensity in the 0 to 0.5 region varies with the experimental geometry while that of 0.5 to 1 does not. For $k_{\|}$ from 0.5 to 1, only one branch (holon) exists and thus one should see only the overall intensity modulation. By contrast, multiple branches are allowed in the 0 to 0.5 region. A relative intensity change resulting from different experimental conditions can induce the shift of the maximum intensity position. Figure 6(c) depicts what would happen to the maximum intensity position if there are matrix element modulations. Therefore, the shift of the maximum intensity position under various measuring conditions for $k_{\|}$ from 0 to 0.5 may be a manifestation of the modulations in the spinon and holon contributions to the excitation spectra. Note that, as discussed before, the maximum intensity position shift is not due to $k_{\perp}$ momentum because two spectra ($\|$, 1 and $\perp$, 0.9) with very similar conditions except the polarization show different dispersions.

Although the spin-charge separation picture advanced above is very consistent with E versus k relationships, the observed behavior in the spectral intensity requires some explanation. In all cases, we found the observed spectral intensity is highest near $k_{\|}=0.5$ which is not a feature in the current theory as shown in Fig. 6. There are two possible explanations for this discrepancy. First, it can be attributed to the photoemission cross-section effect. It is well known that the lowest excitation feature has Cu $3d_{x^2-y^2}$ character in a planar CuO_4 structure. However, due to hybridization between O $2p$ and Cu $3d$, the feature has a finite amount of O $2p$ character. This mixing has a momentum dependence.[24] It is empirically known that the photoemission cross section of O $2p$ is much larger than that of Cu $3d$.[23] Therefore, the more the feature has O $2p$ character, the higher the cross section is. Figure 7(a) shows the results on 16 site Cu-O ring. The parameters used are $T_{\mathrm{pd}}=1$, $\Delta=3$, and $U_d=8$. The red curve shows the O $2p$ contribution and the blue curve the Cu $3d$ contribution. It is clear from this figure that the low excitation energy feature near $k=0$ is dominated by Cu $3d$ while the feature near $k=0.5$ has contributions from both O $2p$ and Cu $3d$. Panel b of the figure shows the spectrum after the cross section effect has been considered. Even though it has finite-size effects, it reasonably explains the intensity change between k of 0 and 0.5.

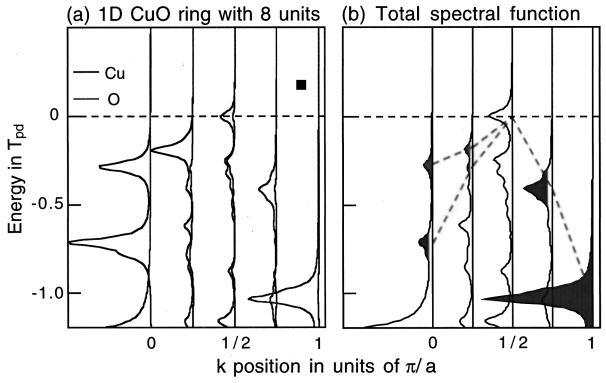

FIG. 7. (a) The calculated O $2p$ and Cu $3d$ spectral function in a CuO ring of 8 units (16 sites). The parameters used in the calculation are $T_{\mathrm{pd}}=1$, $\Delta=3$, and $U_d=8$. T_{pd}, Δ, and U_d are O $2p$-Cu $3d$ hopping, charge transfer, and Cu $3d$ on-site Coulomb repulsion energies, respectively. The red curve shows the contribution from O $2p$ and blue from Cu $3d$. (b) The total spectral function after the cross-section effect is considered. The spinon (shaded in red) and holon (shaded in blue) branches are seen as well as higher-energy incoherent peaks. The large peak at $k=1$ with holon character cannot be observed since it is buried in the main valence peak. This has more finite-size effect, but the overall dispersion (dashed lines) is similar to that in Fig. 6.

Second, our simulation indicates that the introduction of next-nearest-neighbor interaction J' qualitatively improves the agreement between the theory and the experiment. This effect originates from the fact that J' introduces frustrations that damp the spinon excitations. As a result, spectral weight of the spinon branch is suppressed and some of the weight away from $k_{\|}=0.5$ is pushed to higher-energy incoherent excitations that cannot be observed in the experiments. On the other hand, this introduction of J' has less effect on the E versus k relationships of the spinon and holon branches.

In light of above discussions, the most important point of the data in Fig. 4 is that, despite the complication of the matrix elements, the data showed a strong evidence for multiple bands in $k_{\|}=0$ to 0.5 region but single band for $k_{\|}=0.5$ to 1. This is exactly what one would expect as the direct consequences of the spin-charge separation. The J' consideration would also suppress the intensity of the spinon branch in general, leading to a stronger relative intensity for the holon branch. We note that the spinon branch should have smaller bandwidth than the band with the smallest width in Fig. 5 because of the holon contribution. Taking above discussions as a whole, the ARPES data from $SrCuO_2$ can be best interpreted by the spin-charge separation. At this point, it is worth noting that one should see the light particle (holon scaled by t) more clearly in one dimension than in two dimensions, where the hole motion is more strongly

coupled to the spin system. Thus it should be much harder to see the light holon band in two dimensions even when it exists.

Our results can be explained in an intuitive way. As depicted in Fig. 1, removal of an electron from the chain leaves a hole behind whose propagation is responsible for the dispersions seen in ARPES. The propagation of the photohole in the 1D chain turns into two ''topological defects'' in the AF chain. The first is the spin misalignment defect labeled S whose propagation is scaled by the restoring energy J. The second is the hole defect labeled H whose propagation is scaled by the hopping energy t. These defects can be regarded as spinons and holons. From this, we can see that the injected photohole ''decays'' into a spinon and holon.[25] Energy- and momentum-conservation laws enforce the following energy and momentum relationships between the spinon, the holon, and the photohole:

$$k = k_h - k_s \ \text{(momentum conservation)},$$

$$E = E_h - E_s \ \text{(energy conservation)},$$

where k, k_s, k_h, E, E_s, and E_h are momenta and energies of the photohole, spinon, and holon, respectively. The different signs on spinon and holon parts are due to the fact that the photoemission process corresponds to creation of a holon and annihilation of a spinon.

Figures 8(a) and 8(b) illustrate the dispersion relations for the holon and spinon branches, respectively, scaled in width by $2t$ and $\pi J/2$ as indicated by theoretical analysis.[26] For a spin chain with an AF interaction at half filling as in $SrCuO_2$, the holon band is empty while the spinon band is half filled and has the ''Fermi surface.'' To create the lowest-energy excitation, one can create the lowest-energy holon at $k_h = 1$ and annihilate a spinon at the Fermi surface with $k_s = 1.5$ (two circles in the figure). Then the momentum of the photohole becomes $k = -0.5$ (this corresponds to photoelectron momentum of $k_\parallel = 0.5$ in the figure) at which we observe the maximum of the bands in photoemission. Similar analysis leads to the expected picture in Fig. 8(c). The reason that only one band with holon character exists between 0.5 and 1 is that the spinon band is half filled. From 0 to 0.5, we have a heavily shaded region where strong photoemission signal is expected. This region is bounded by the spinon branch at lower excitation energy and holon branch at higher excitation energy. This result is in accord with the rigorous results presented in Fig. 6(a). The exact solution in Fig. 6(a) shows that the edges tend to have higher spectral intensities. It is clear from remarkable similarity between the theoretical picture in Fig. 8(c) and the data set in Fig. 5 that the spin-charge separation is the natural explanation of the experimental data from $SrCuO_2$, which sharply contrast with anything one expects from the conventional band picture.

Another important aspect of these results is that this is the first direct observation of spinons. Even though studies on AF spin chains date back to the early 1930's,[28] only in the 1980's was it realized that the elementary magnetic excitation in the system is not a spin wave with spin 1. Rather it is an excitation with spin 1/2, now called a spinon.[29,30] However, it has not been observed directly due to the fact that only two spinon excitations, that is, spin waves, are allowed,

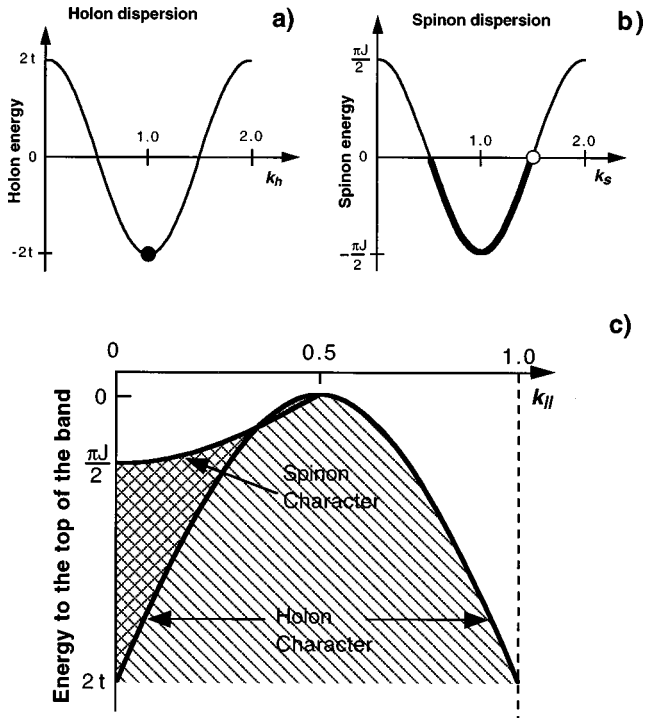

FIG. 8. (a) and (b) Dispersions for holon and spinon. The holon band is empty while the spinon band is half filled and has the Fermi surface. (c) The photoemission spectrum obtained from the two dispersions and the energy- and momentum-conservation equations. In the region between 0 and 0.5, there are two boundary bands with the bandwidths scaled by J and t. The band with width $\pi J/2$ is due to spinon dispersion and the band with $2t$ is due to holon dispersion. Spectra in the shaded region show mixed excitations of spinons and holons. In the region between 0 and 0.5, strong spectral intensity is expected.

for example, in neutron diffraction experiments.[31] The direct observation of holon and spinon branches in the data proves that these are indeed new elementary particles with well-defined energy versus momentum relationships.

In summary, an ARPES study of 1D $SrCuO_2$ reveals a phenomenon that cannot be reconciled with the conventional band picture. Using a many-body t-J model without free parameters, both rigorous numerical calculation and intuitive analysis invoking the spinon and holon concepts can naturally explain the experimental data. The finding is not only a demonstration of the spin-charge separation in 1D $SrCuO_2$ but also direct observation of new elementary particles in a solid.

We acknowledge the stimulating discussion with R. Laughlin, P. W. Anderson, and T. Mizokawa, and thank P. Blaha for the local density approximation (LDA) results. This work was supported by the U. S. DOE, office of Basic Energy Science, Division of Material Science, NEDO, and the Ministry of Education, Science and Culture of Japan. Stanford Synchrotron Radiation Laboratory is operated by the U. S. DOE, office of Basic Energy Sciences, Division of Chemical Sciences. The computation was done using the facilities of the supercomputer center, the the Institute of Solid State Physics, University of Tokyo.

*Present address: Press Warehouse, CMR, 435 Santa Teresa Street, Stanford, CA 94305-4045.

†Present address: Institute for Materials Research, Tohoku University, Sendai 980-77, Japan.

[1] E. H. Lieb and F. Y. Wu, Phys. Rev. Lett. **20**, 1445 (1968).

[2] G. D. Mahan, *Many-Particle Physics* (Plenum Press, New York, 1990).

[3] Z. Zou and P. W. Anderson, Phys. Rev. B **37**, 627 (1988).

[4] P. W. Anderson, *A Career in Theoretical Physics*, World Scientific Series in 20th Century Physics Vol. 7 (World Scientific, Singapore, 1994).

[5] V. J. Emery, S. A. Kivelson, and O. Zachar (unpublished).

[6] J. W. Allen, G.-H. Gweon, R. Claessen, and K. Matho, J. Phys. Chem. Solids **56**, 1849 (1995); R. Claessen, G.-H. Gweon, F. Reinert, J. W. Allen, W. P. Ellis, Z.-X. Shen, C. G. Olson, L. F. Schneemeyer, and F. Levy, J. Electron Spectrosc. Relat. Phenom. **76**, 121 (1995).

[7] B. Dardel, D. Malterre, M. Grioni, P. Weibel, Y. Baer, and F. Levy, Phys. Rev. Lett. **67**, 3144 (1991).

[8] A. Sekiyama, A. Fujimori, S. Aonuma, H. Sawa, and R. Kato, Phys. Rev. B **51**, 13 899 (1995); M. Nakamura, M. Nakamura, A. Sekiyama, H. Namatame, A. Fujimori, H. Yoshihara, T. Ohtani, A. Misu, and M. Takano, *ibid.* **49**, 16 191 (1994).

[9] Certain behaviors of spin and charge motions have been observed in 1D polyacetylene, as summarized by Heeger *et al.* in Rev. Mod. Phys. **60**, 781 (1988). However, those behaviors are driven by electron-phonon interaction, and are different from the correlation driven spin-charge separation discussed here.

[10] Theoretical calculation predicts that the spin-charge separation effect is most pronounced when we study the behavior of a hole in an insulator when correlation is similar. Since the photoemission process studies the behavior of a photo hole, the situation is ideal to observe the spin-charge separation.

[11] C. Kim, A. Y. Matsuura, Z.-X. Shen, N. Motoyama, H. Eisaki, S. Uchida, T. Tohyama, and S. Maekawa, Phys. Rev. Lett. **77**, 4054 (1996).

[12] B. O. Wells, Z.-X. Shen, A. Y. Matsuura, D. M. King, M. A. Kastner, M. Greven, and R. J. Birgeneau, Phys. Rev. Lett. **74**, 964 (1995).

[13] N. Motoyama, H. Eisaki, and S. Uchida, Phys. Rev. Lett. **76**, 3212 (1996).

[14] M. Takigawa *et al.* (unpublished).

[15] Z.-X. Shen and D. S. Dessau, Phys. Rep. **253**, 1 (1995).

[16] It is worth pointing out that this turns out to work only for the $k_{\|}$ values between 0.5 and 1.

[17] N. F. Mott, *Metal-Insulator Transitions* (Taylor and Francis LTD., London, 1974).

[18] Here, one has to note that the band width in 1D alone does not prove the spin-charge separation discussed in the text as other experiments on 1D showed rather peculiar E versus k relationship (Ref. 6). In fact, the underlying holon dispersion between 0 and 0.5 is very similar to what the band calculation based on LDA predicts (Ref. 19). This is expected since the motion of a holon should be determined by t which the LDA based band calculation should predict very well. The peculiarity is with the bandwidth of the 2D where more than 2 eV bandwidth is predicted by LDA calculation while the experimental band width is only 0.3 eV (Ref. 12). This is believed to be due to the strong interaction between a hole and the spin background. Therefore, it should be the comparison of the results from 1D and 2D systems with similar Cu-O-Cu bonds that proves the decoupling of the charge motion from the magnetic excitation in one dimension.

[19] P. Blaha (private communication).

[20] H. Suzuura, H. Yasuhara, A. Furusaki, N. Nagaosa, and Y. Tokura, Phys. Rev. Lett. **76**, 2579 (1996); H. Yasuhara *et al.* (unpublished).

[21] For exact diagonalization, refer to T. Tohyama and S. Maekawa, J. Phys. Soc. Jpn. **65**, 1902 (1996).

[22] It is not well understood why the peaks are broad. Even in 2D, peaks tend to get broader as we go to lower doping, that is, away from the Fermi liquid. Our calculation shows that the next-nearest-neighbor interactions that are introduced to explain the behavior of the spectral intensity also tend to broaden the features. The interchain coupling certainly has contribution to the broad features. But it is not clear at this stage whether the broadness of the features is entirely due to the next-nearest-neighbor interactions and the interchain coupling.

[23] It was initially pointed out by Sawatzky *et al.* [Phys. Rev. B **20**, 1546 (1979)] that the calculated atomic cross section should be multiplied by 3 to reproduce the whole valence-band spectra of the $3d$ transition-metal oxides for Mg $K\alpha$ ($h\nu = 1.25$ keV). It was later found that this holds true for low photon energies such as $h\nu = 20$ eV (private communication with T. Mizokawa). If we consider the fact that Cu and O are mostly in their $3d^9$ and $2p^6$ states, their cross-section ratio becomes approximately 10. For the calculated atomic cross sections, refer to J.-J. Yeh, *Atomic Calculation of Photoionization Cross-sections and Asymmetry Parameters* (Gordon and Breach Science, Langhorne, 1993).

[24] J. J. M. Pothuizen, R. Eder, N. T. Hien, M. Matoba, A. A. Menovsky, and G. A. Sawatzky, Phys. Rev. Lett. **78**, 717 (1997).

[25] To be exact, an electron should be regarded as spinless charge and a spinon. Therefore, a hole consists of a holon and an antispinon (or spinon hole). This is the reason why the creation of a hole corresponds to creation of a holon and annihilation of a spinon.

[26] These relations have been derived from the following theoretical analyses: (i) In the limit of $J/t \rightarrow 0$, the Hamiltonian is decoupled into the spin and charge parts (see Ref. 27), and (ii) the spin part is mapped onto a system of interacting spinless fermions after the Jordan-Wigner transformation.

[27] M. Ogata and H. Shiba, Phys. Rev. B **41**, 2326 (1990); S. Sorella and A. Parola, J. Phys.: Condens. Matter **4**, 3589 (1992).

[28] H. A. Bethe, Z. Phys. **71**, 205 (1931).

[29] L. D. Faddeev and L. A. Takhtajan, Phys. Lett. **85A**, 375 (1981).

[30] D. M. Haldane, Phys. Rev. Lett. **60**, 635 (1988); B. S. Shastry, *ibid.* **60**, 639 (1988).

[31] D. A. Tennant *et al.*, Phys. Rev. B **52**, 13 368 (1995).